Visible Light-Driven Dye-Sensitized Photocatalytic Hydrogen Production by Porphyrin and its Cyclic Dimer and Trimer: Effect of Multi-Pyridyl-Anchoring Groups on Photocatalytic Activity and Stability

Motonori Watanabe,*,† Songmei Sun,† Tatsumi Ishihara,†,‡ Takuya Kamimura,§ Masato Nishimura,§ and Fumito Tani*,§

†International Institute for Carbon Neutral Energy Research, Kyushu University, 744 Motooka, Nishi-ku, Fukuoka 819-0395, Japan

‡Department of Applied Chemistry, Faculty of Engineering, Kyushu University, Nishi-ku, Fukuoka 819-0395, Japan

§Institute for Materials Chemistry and Engineering, Kyushu University, 744 Motooka, Nishi-ku, Fukuoka 819-0395, Japan

* Supporting Information

ABSTRACT: The monomer, dimer, and trimer of 5,15-diphenyl-10,20-di(pyridin-4-yl)porphyrin are used to investigate the multi-anchoring effect on TiO_2 for visible light-driven photocatalytic hydrogen production in a water medium. Further, the porphyrin trimer is prepared and analyzed by nuclear magnetic resonance (NMR) spectroscopy, absorption spectroscopy, electrochemical voltammetry, fast atom bombardment (FAB) mass spectroscopy, and density functional theory (DFT) computation. The results of this study indicate that the peak intensities of the absorption spectra increase as the number of porphyrin units increases, while changes could be barely observed in the highest occupied molecular orbital (HOMO)−lowest unoccupied molecular orbital (LUMO) gaps. The porphyrin dimer in a 1 wt % Pt-loaded TiO_2 powder photocatalyst system exhibited optimal hydrogen production performance in a stable state over a period of 80 h and at a superior rate of 1023 μmol·g^{-1}·h^{-1}. Further, the stability of the photocatalytic system was systematically investigated using films containing dyes on 1 wt % Pt-loaded TiO_2/FTO. For a film containing the dimer, almost no change was observed in the hydrogen-bond coordination mode of the dimer and the photocurrent during the photocatalytic reaction. However, the photocurrents of the monomer and trimer were altered during visible light irradiation without altering the coordination mode, indicating that the arrangements and orientations of the porphyrins on TiO_2 surfaces were altered. These results indicate that the presence of multiple anchoring groups enhance the stability of the photocatalytic system and the rate of hydrogen production.

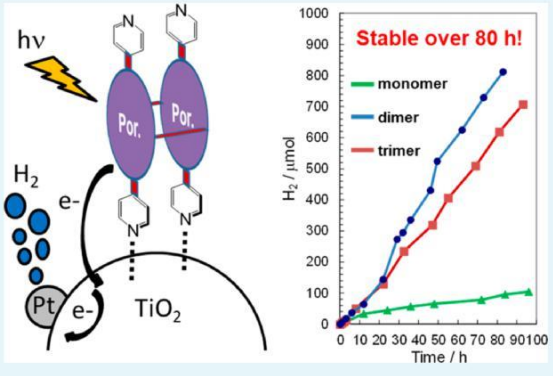

KEYWORDS: dye-sensitized, hydrogen production, photocatalysis, porphyrin, pyridyl anchor

INTRODUCTION

The dye-sensitized photocatalysts that are responsive to visible light are useful for directly harvesting sunlight to generate energy. This type of system has been extensively studied, resulting in the development of photocatalytic combination systems, including TiO_2,[1−4] SnO_2,[5] ZnO,[6] CuO,[7] $KTaO_3$,[8−10] TaON,[11] ZnO:GaN,[12] BiOCl,[13] Nb-based oxide nanosheets,[14−17] reduced graphene oxide,[18−22] and C_3N_4.[23−25] In dye-sensitized photocatalysts, the dyes are excited by light energy, which further inject the excited electrons into the bulk/surface of the photocatalyst.[26] The electrons can be used for performing photosynthesis at the active site of the photocatalyst, recombining electrons into organic dyes, or releasing energy. The charge that arrives at the surface must exhibit a sufficient lifetime for efficiently generating hydrogen. Therefore, one of the most important issues related to a dye-sensitized photocatalyst is determining the manner in which the charge separation at the interface of the dye/photocatalyst system can be increased. Further, modifying the dye is an effective method for transferring electrons from the dye to the photocatalyst. Several studies have investigated efficient light absorption systems; for example, π-conjugated systems, such as phthalocyanines,[27−29] xanthene dyes,[30−33] donor−acceptor type systems,[26,34] and metal−ligand charge transfer type dyes, including ruthenium complexes,[35] exhibit an extensive visible absorption band for ensuring that efficient light absorption can be achieved with respect to charge transfer to the photocatalyst. Further, the electrons are mostly used in an

efficient manner at the hydrogen generation site of the photocatalyst if the lifetime of the charge separation state between the dye and the catalyst is considerably long, and this can be accomplished by inserting a π-conjugated system into the dye structure.[36] The collection of electrons for hydrogen production in dye-supported photocatalysts can also be controlled by modifying the dye using hydrophilic or hydrophobic substituents. Lee et al.[37] and our research group[38] have illustrated that electrons can be efficiently injected into the hydrogen production site by introducing a hydrophobic substituent in the dye. The hydrophobic substituent treatment of the dye could improve the hydrophobicity of the photocatalyst surface and suppress the photoinduced electron trapping at the interface between the solvent and the dye-photocatalyst.[38] Han et al. reported that the presence of a hydrophilic substituent in the dye decreased the charge recombination rate that was observed in the excited state because of the interactions between the hydrophilic group and the water medium.[39] However, ensuring a stable supply of the charge injection cycle (from the dye to the photocatalyst) is important from the viewpoint of improving the durability of the photocatalyst. Further, a usual dye-sensitized type photocatalytic system contains an electron donor site and an anchor site for attaching onto the photocatalyst. Carboxylic acid,[30−33,40] cyanocarboxylic acid, [41−44] phosphoric acid,[45−47] and hydroxyl groups[48,49] have all been employed as anchors. Additionally, a multianchoring system with several charge transfer sites has also been reported, with phenol[50] and phosphoric acid[51] serving as anchors. Because these anchor sites can be hydrolyzed under the dye-sensitized type photocatalytic reaction conditions,[50] the photocatalytic activity is only maintained for a period of 10−20 h.[26,52] Abbotto et al. investigated the bridge effect of organic dyes with dianchored thiophene cyanocarboxylic acid groups and reported that the modification of the thiophene moiety affected the stability of their photocatalytic activity. On the TiO_2 surface, these dyes exhibited a highly stable photocatalytic activity over a period of 20−90 h and a turnover frequency of 250 $\mu mol \cdot g^{-1} \cdot h^{-1}$.[53] These results indicated that anchoring groups enhanced the dye stability of the metal oxide surface in case of photocatalytic reactions. Further, the pyridyl groups are considered to be a potential candidate to serve as an effective anchor group for the metal oxide surfaces in the dye-sensitized solar-energy conversion systems.[54] This type of anchor group can coordinate with the metal oxide through Brønsted or Lewis acid-type coordination. Liu et al. reported the use of stable perylene dye-sensitized TiO_2 photocatalysts containing pyr-idine groups.[55] Ozawa et al. reported that dyes containing pyridyl groups could remain active for more than 120 min, even in systems that are applied to photoelectrodes.[56] However, there is insufficient evidence related to the pyridyl group's high level of stability that is observed during photocatalytic reaction. Because the porphyrin dye exhibits a wide absorption in the visible light spectrum, it demonstrates photocatalytic hydrogen production when it is stimulated with visible light.[57,58] Further, supramolecular porphyrin nanowire has also displayed effective charge separation under visible light between nanowire and Pt cocatalyst, resulting in an effective hydrogen evolution rate that is as high as 14600 $\mu mol \cdot g^{-1} \cdot h^{-1}$ over a period of 40 h.[59] It has been reported that a porphyrin dye exhibits photocatalytic activity even when it is combined with a semiconductor material. For example, when 5,10,15,20-tetrakis(4-(hydroxyl)phenyl) porphyrin (TPPH) or Zn(II)-5,10,15,20-tetrakis(4-N-methylpyridyl)porphyrin ($[ZnTMPyP]^{4+}$) are loaded on the reduced graphene oxide (RGO) with a donor−acceptor type interaction, a rate of 2240 $\mu mol \cdot g^{-1} \cdot h^{-1}$ over 5 h[60] and a rate of 2560 $\mu mol \cdot g^{-1} \cdot h^{-1}$ over 24 h have been achieved for TPPH-Pt/RGO.[61] Noncovalent type μ-oxo-bis-iron(III) porphyrin ($(FeTPP)_2O$)-loaded C_3N_4 and 5,10,15,20-Tetrakis (4-carboxyphenyl) porphyrin (TCPP)-loaded Pt/C_3N_4 produced 59.2 μmol after 4 h[62] and a production rate of 1208 $\mu mol \cdot g^{-1} \cdot h^{-1}$ over 25 h.[63] (Zinc-5-(4-carboxyphenyl)-10,15,20-tri(3-pridyl)porphyrin (ZnMT3PyP)-loaded Pt/C_3N_4 displayed a stable hydrogen productivity of 400 $\mu mol \cdot h^{-1}$ over a period of 10 h.[64] Zn(II)-tetrakis(4-carboxyphenyl)porphyrin (ZnTCPP)-anchored MoS_2/TiO_2 displayed a photocatalytic hydrogen production of approximately 160 μmol after 36 h even though the production rate gradually degraded after 2−4 h.[65] ZnTCPP/MoS_2/ZnO showed 75 $\mu mol \cdot g^{-1} \cdot h^{-1}$ after 3 h.[66] 5,15-diphenyl-10,20-di(4-pyridyl)porphyrin (DPyP) included a pyridyl group-anchored metal-loaded graphene oxide, which enhanced the stability of photocatalytic hydrogen production. This system maintained a photocatalytic production rate of 116 $\mu mol \cdot g^{-1} \cdot h^{-1}$ over 8 h.[22] Therefore, more efficient and stable dye-sensitized photocatalyst systems can be constructed using porphyrin units that incorporate multiple pyridyl groups to promote hydrogen bonding with the acidic sites in semiconductors. Tani et al. reported the photochemical dynamics and activity of the cyclic porphyrin dimer.[67−71]

The porphyrin units are bonded through diacetylene or other π-conjugated systems to produce rigid structures. The dimer can be used to create an effective electrochemical catalyst,[72] photoinduced charge separation for photovol-taics,[73,74] and singlet oxygen production.[75] It has also been reported that the pyridyl groups of the dimer could be chemically adsorbed through Brønsted acid hydrogen bonding onto the surface of TiO_2 and that the resulting system acted as a dye-sensitized solar cell.[76] This unique system is not only expected to increase the efficiency of charge transfer but is also expected to increase the chemical stability of the dye because of multiple pyridyl groups that provide hydrogen bonds to the TiO_2 surface. This study examines the hydrogen generation reaction of the dye-sensitized photocatalysts containing porphyrins with multiple pyridyl groups (Figure 1). The monomer (1), cyclic dimer (2), and trimer (3) of 5,15-diphenyl-10,20-di(pyridin-4-yl)porphyrin were investigated as dye-sensitizers in novel highly stable photocatalytic hydrogen production systems.

RESULTS AND DISCUSSION

Synthesis and Physical Properties of Dyes 1−3. The dyes, monomer 1, and dimer 2, were synthesized using the methods reported in previous studies.[67,68,77] Further, the porphyrin macrocyclic trimer was obtained using a reported method with a few modifications (Scheme 1).[67,68,76] Zinc(II) 5,15-bis(3-ethynylphenyl)-10,20-di(pyridin-4-yl)porphyrin (5) was cyclized by Glaser-coupling with CuCl in pyridine, which was followed by treatment with hydrochloric acid to eliminate zinc from the porphyrin core for generating free-base macrocyclic trimer 3 in a 20% yield. The structure of macrocycle 3 was confirmed by ^1H nuclear magnetic resonance (NMR) spectroscopy and fast atom bombardment mass spectrometry (FAB-MS). The high-resolution FAB-MS spec-trum indicated a molecular ion signal at m/z 1987.6728 (M +

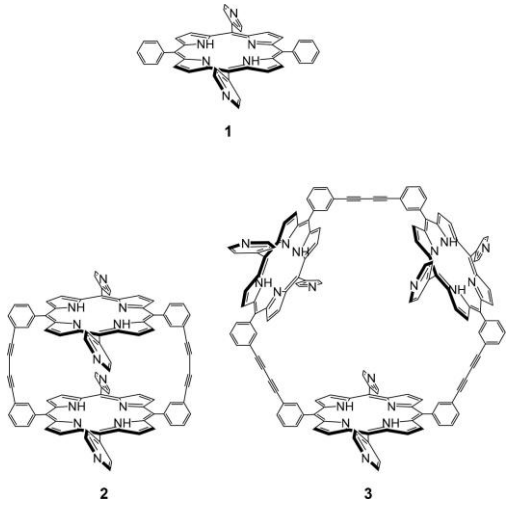

Figure 1. Molecular structure of porphyrin monomer 1, dimer 2, and trimer 3.

Scheme 1. Synthesis of Cyclic Porphyrin Trimer 3

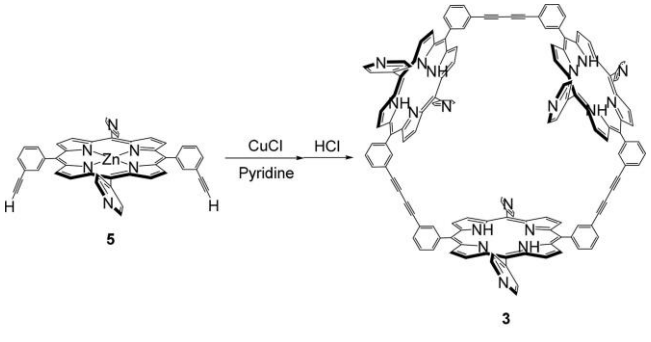

H^+, calculated 1987.6735 error = −0.4 ppm), which corresponds to that of 3.

The absorption spectra of 1−3 were measured in a 1,1,2,2-tetrachloroethane solution (Figure 2a). In the solution, dye 3

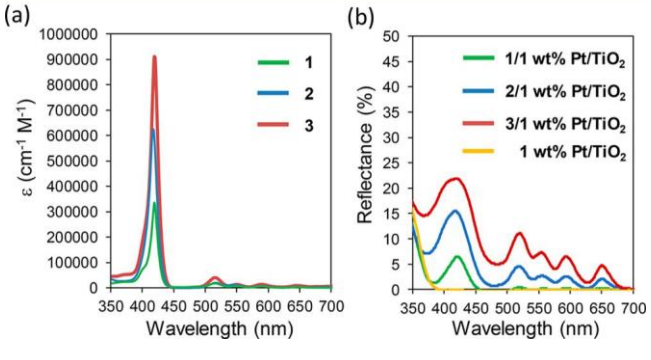

Figure 2. (a) Absorption spectra of porphyrin monomer 1, dimer 2, and trimer 3 in a 1,1,2,2-tetrachloroethane solution. (b) The diffuse reflectance spectra of dyes 1−3 on 1 wt % Pt-loaded TiO_2 and 1 wt % Pt-loaded TiO_2 catalyst.

exhibited a characteristic Soret band at 420 nm (ε = 908064) and four Q-bands at 516 (ε = 40323), 550 (ε = 14516), 589 (ε = 14516), and 645 nm (ε = 4677). The absorption bands for 1 were observed at 419 (ε = 335151), 516 (ε = 17036), 550 (ε = 6473), 589 (ε = 5337), and 645 nm (ε = 3180), whereas those for 2 were observed at 417 (ε = 623894), 516 (ε = 20353), 545 (ε = 12389), 590 (ε = 7080), and 647 nm (ε = 4425). The absorption intensities of 1 and 2 were observed to be similar to the values that were reported in the literature.[67,77]

The absorption intensity at the Soret band in 3 was approximately three times higher than that of monomer 1, indicating that the porphyrin in the trimer did not communicate effectively via intramolecular interactions. The HOMOs and LUMOs of 1−3 were estimated using difference pulse voltammetry in 1,1,2,2-tetrachloroethane containing 0.1 M nBu_4NPF_6 (Figure S1). Further, the oxidation and reduction peaks were observed at +1.11 V (vs NHE) and −1.02 V (vs NHE) for 1, +1.11 V (vs NHE), and −1.02 V (vs NHE) for 2, and +1.08 V (vs NHE) and −0.98 V (vs NHE) for 3, respectively.

To estimate the geometries and HOMO−LUMO energies of 1−3, the density functional theory (DFT) computation were performed at the B3LYP/6-31G(d) level using Gaussian 16 (Figure 3). Further, the porphyrin moieties of 2 and 3 connected with the diacetylene unit and retained the same structure as that of 1. On the basis of the HOMO and LUMO of all the three dyes, the orbitals were delocalized only over the porphyrin units, and no orbitals were observed on the acetylene units in 2 and 3, indicating that the intramolecular interactions in the porphyrin units were weak. These estimations were in-line with the experimental absorption spectra in the solution, while the weak interaction between the porphyrin units of the dimer was confirmed by our previous studies.[67,75,76] The energy gaps of the dyes were 2.73 eV for 1, 2.69 eV for 2, and 2.71 eV for 3. The observed trends in these values were observed to be consistent with the experimental energy gaps that were measured using difference pulse voltammetry. The similar absorption structures and increasing molar absorption coefficients at the Soret and Q-bands with increasing porphyrin units indicated that the porphyrin units in the macromolecule acted independently as photosensitizers.

Figure 2b depicts the diffuse reflectance spectra of the dye-adsorbed 1 wt % platinum (Pt) coloaded titanium oxide (anatase TiO_2) catalyst. The 1 wt % Pt coloaded TiO_2 powder did not demonstrate much reflectance in the visible light range. After dyes 1−3 were loaded on the catalyst, new bands were observed at more than 350 nm, with peaks being observed at 422, 520, 557, 595, and 645 nm for 1, at 423, 523, 553, 594, and 656 nm for 2, and at 420, 519, 557, 595, and 648 nm for 3. These peaks were virtually identical to those observed in the solution-state absorption spectra, while the observed Soret band reflectance intensity was broad in the solution state, indicating that the orientation on the TiO_2 surface was affected by the electronic interaction between the dye and TiO_2 or between the dyes themselves. The amount of dye-loading was determined by the decrease in the Soret band intensity of the solution by adsorbing the dye to TiO_2. The dye-loading of 1−3 on TiO_2 were 8.2 μmol/g for 1, 28.3 μmol/g for 2, and 30.1 μmol/g for 3. The values for 2 and 3 were similar to that of the cyanocarboxylic acid group-loading (30 μmol/g).[36] Dye 1 was expected to weakly interact with TiO_2 based on the amount of dye loading. All the three dyes displayed a hydrogen bonding-type interaction between the pyridyl group of dyes and TiO_2 (discussed later), which indicated that the porphyrin moiety was arranged on the TiO_2 surface with the pyridyl group as the anchor site. Further, an undesirable orientation (porphyrin ring lying flat on the TiO_2 surface) was expected because of the nonbulky structure of 1. However, dyes 2 and 3 displayed a considerably higher loading than that displayed by 1, indicating a more tightly packed orientation on the TiO_2 surface. By

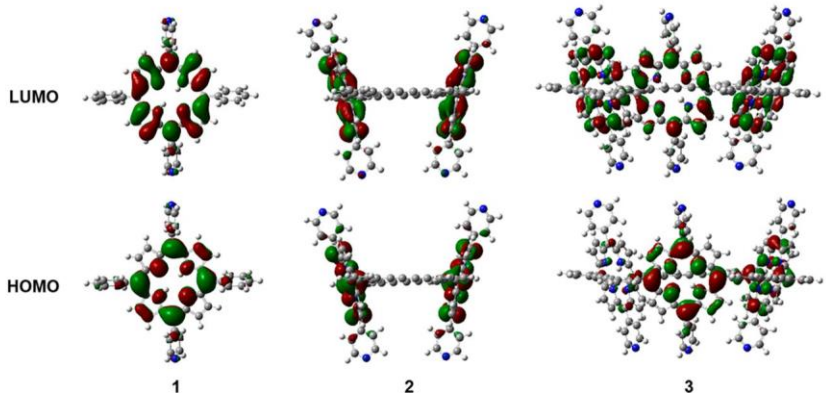

Figure 3. Molecular orbitals of HOMO and LUMO from the optimized structures of 1−3 at the B3LYP/6-31G(d) level of theory.

measuring the amount of N_2 gas adsorption, the Brunauer−Emmett−Teller (BET) surface areas were determined to be 53.1 m^2/g for 1/1 wt % Pt/TiO_2, 54.0 m^2/g for 2/1 wt % Pt/TiO_2, 54.9 m^2/g for 3/1 wt % Pt/TiO_2, 55.9 m^2/g for 1 wt % Pt/TiO_2, and 56.9 m^2/g for pure TiO_2. Compared with 1 wt % Pt/TiO_2 and pure TiO_2, the adsorption sites of N_2 molecule were decreased in the cases of the dye/Pt/TiO_2 systems, suggesting that the dyes were actually loaded on TiO_2 surfaces.[22]

Further, the structures of dyes 2 and 3 were macrocyclic and were expected to be arranged perpendicular to the TiO_2 surface by hydrogen bonding through the pyridyl groups. When the porphyrin unit is vertically arranged on TiO_2, it should be tightly packed against the TiO_2 surface, which would explain the increase in the amount of dye loading in 2 and 3 as compared to that observed in 1. On the basis of the experimental results, we confirmed that all the dye LUMOs contained higher energy (−0.98 to −1.02 V vs NHE) than that contained in the conduction band of anatase TiO_2 (−0.5 V NHE, Figure 4). This indicated that electrons can be injected

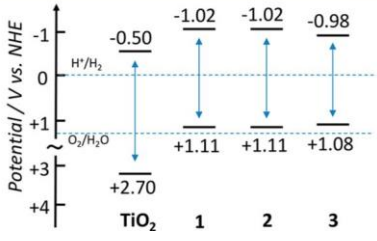

Figure 4. Energy diagram of TiO_2 and the porphyrin dyes 1−3.

into the TiO_2 surface from dyes 1−3 under light irradiation. The physical properties of all the three dyes are summarized in Table 1

Visible Light-Driven Photocatalytic Hydrogen Production Test. The visible light-driven photocatalytic hydrogen production in water medium using 1−3/1 wt % Pt/anatase TiO_2 nanoparticles was investigated. The dye-loaded 1 wt % Pt/TiO_2 catalyst powder was suspended in water with ascorbic acid (pH 4) acting as a sacrificial reagent. This suspension was purged with argon, and a Xe lamp (>420 nm filter) was used to irradiate the system. Further, the amount of hydrogen gas output was measured using gas chromatography (Figure 5). Dye 1 displayed hydrogen production over a period of 80 h although the production activity decreased after 10 h. In contrast, dyes 2 and 3 exhibited linear hydrogen productivity over an 80-h period. These results indicated that the multi-4-pyridyl anchor for the porphyrin dye-sensitized photocatalytic hydrogen production system was observed to be highly stable under the reaction conditions. Notably, the hydrogen production rates of 2/1 wt % Pt/TiO_2 (1023 μmol·g^{-1}·h^{-1}) and 3/1 wt % Pt/TiO_2 (761 μmol·g^{-1}·h^{-1}) were considerably higher than that of 1/1 wt % Pt/TiO_2 (102 μmol·g^{-1}·h^{-1}). Controlled experiments using TiO_2 and 1 wt % Pt-loaded TiO_2 for hydrogen production under visible light (>420 nm) demonstrated hydrogen production rates of 0 and 12 μmol·g^{-1}·h^{-1}, respectively. This drastic increase in the hydrogen productivity of the dye-loaded photocatalysts indicated the occurrence of the dye-sensitized type visible light-driven photocatalytic reaction. To evaluate the catalytic activity for hydrogen production in these systems, the turnover numbers (TON) per porphyrin unit were determined (Figure S2). The 2/1 wt % Pt/TiO_2 dye exhibited a higher TON (2860 after 83 h) as compared to that exhibited by 3/1 wt % Pt/TiO_2 (1370 after 81 h) and 1/1 wt % Pt/TiO_2 (1980 after 84 h). Although the physical properties and DFT results indicated that the porphyrin units in dimer 2 and trimer 3 acted independently as photosensitizers, dye 2 was the most active sensitizer for the production of hydrogen because of the efficient injection of electrons from 2 into the surface of TiO_2 under visible light, which was confirmed by the photocurrent experiment (discussed later). Following the completion of the photoreaction, the solution was extracted with 1,1,2,2-tetrachloroethane, and the absorption spectra were measured (Figure S3); further, the peak that was observed at approximately 420 nm remained intact. The amounts of organic dye dissociation after the reaction were estimated to be low for all the three dyes: 1 (26.7 × 10^{-2}%), 2 (1.13 × 10^{-2}%), and 3 (0.73 × 10^{-2}%). This indicated that the porphyrin dyes remained on the TiO_2 surface after the completion of the photoreaction. Further-more, the dissociation amounts of dimer 2 and trimer 3 were substantially lower than that of 1, which indicated that the multianchoring pyridyl system improved the stability of the photocatalyst system.

Absorption Spectra and IR Spectra after the Hydrogen Production Reaction. To further investigate the difference between the hydrogen production rates for 1−3, a thin film of dye/1 wt % Pt-loaded TiO_2 substrate was prepared on fluorine-doped tin oxide (FTO) glass for performing spectroscopic analysis. Figure S4 depicts the dye-adsorbed 1 wt % platinum (Pt) coloaded titanium oxide (anatase TiO_2) films on FTO glass. Because of the difference in the state of the

Table 1. Physical Properties and Calculated Data of Dyes 1−3

sample	abs. at soln.[a] (nm/ε)	reflectance at powder[b] (nm)	loading amount (μmol/g)	oxidation potential[a,c] (V vs NHE)	reduction potential[a,c] (V vs NHE)	energy gap[c] (V)	HOMO[d] (eV)	LUMO[d] (eV)	energy gap[d] (eV)
1	419/335151	422	8.2	+1.11	−1.02	2.13	−5.20	−2.47	2.73
	516/17036	520							
	550/6473	557							
	589/5337	595							
	645/3180	645							
2	417/623894	423	28.3	+1.11	−1.02	2.13	−5.30	−2.61	2.69
	516/20353	523							
	545/12389	553							
	590/7080	594							
	647/442	656							
3	420/908064	420	30.1	+1.08	−0.98	2.06	−5.31	−2.60	2.71
	516/40323	519							
	550/14516	557							
	589/14516	595							
	645/4677	648							

[a]In 1,1,2,2-tetrachloroethane. [b]Dye/1 wt %Pt−TiO_2/FTO. [c]Difference pulse voltammetry was conducted in 0.1 M nBu_4NPF_6 1,1,2,2-tetrachloroethane solution. The potentials were calibrated according to Fc/Fc^+ = +0.63 V vs NHE.[78] [d]Estimated by DFT at the B3LYP/6-31G(d) level of theory.

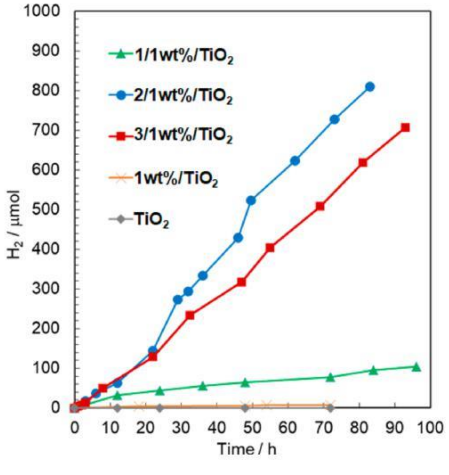

Figure 5. Visible light-driven photocatalytic hydrogen production for TiO_2, 1 wt % Pt-loaded TiO_2, and dyes 1−3 loaded 1 wt % Pt/TiO_2. Conditions: 300 W Xe lamp (>420 nm), ascorbic acid (pH 4) in water.

catalyst, the absorption intensities and the peak positions of the dye on the film were observed to be slightly different from those of the powder. However, the strength and peak position tendencies were observed to be the same for both the powder and film (Figure S4). Furthermore, these peaks were virtually identical to those observed in the solution state absorption spectra, which indicated that it exhibited the same orientation as that exhibited by the powder. The substrates were placed in an aqueous ascorbic acid solution and were irradiated using a Xe lamp. After the initial hydrogen production rate was determined through measurement, the production rate in all the systems was observed to decrease. However, the hydrogen production rate eventually stabilized (Figure S5). The hydrogen production rates of the thin films of 2/1 wt % Pt/TiO_2 and 3/1 wt % Pt/TiO_2 were similar to the rates of 2/1 wt % Pt/TiO_2 and 3/1 wt % Pt/TiO_2 powders.

The absorption spectra of the dyes on 1 wt % Pt−TiO_2 films are presented in Figure 6a−c. Before visible light irradiation, the films of the dyes exhibited characteristic Soret and Q-bands. Before the photoreaction, the Soret band of 1 was

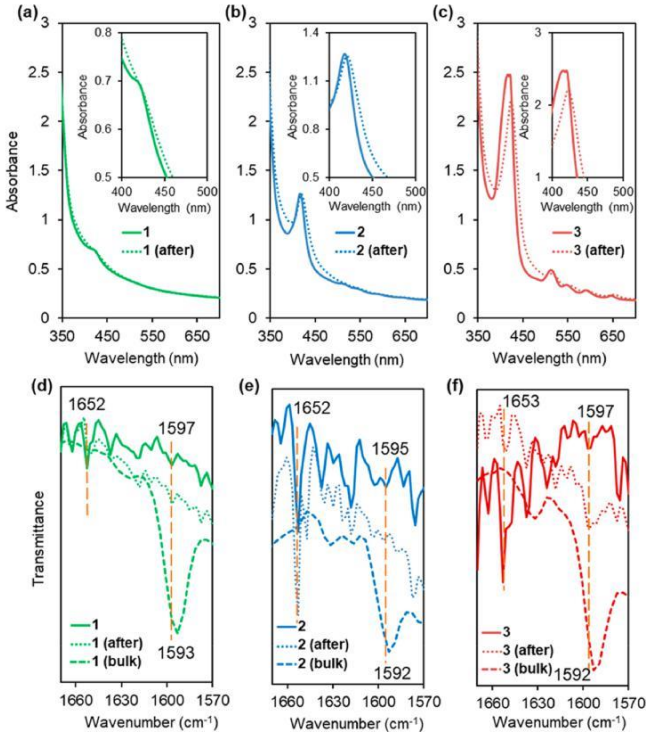

Figure 6. Absorption spectra of dye/1 wt % Pt-loaded TiO_2/ FTO before (solid) and after (dash) visible light-driven hydrogen production: (a) 1, (b) 2, and (c) 3. The FT-IR spectra of the bulk dye (dash) and the catalytic system before (solid) and after (dot) visible light-driven hydrogen production: (d) 1, (e) 2, and (f) 3.

observed to be weak and difficult to confirm because of the small amount of dye loading. After the photoreaction, the Soret band of 1 virtually disappeared because of the broadening that was likely to be caused by the aggregation and orientation change of the porphyrin. As in the case of 1, the Soret band of 3 exhibited a decrease in intensity and red-shift after photoreaction. These changes in absorption spectra indicated that the arrangements and orientations of the porphyrins on the 1 wt % Pt−TiO_2 films varied during the reaction. Further,

2 exhibited almost no change in the intensity and wavelength of the Soret band. This result indicated that dimer 2 was tightly fixed on 1 wt % Pt−TiO_2 film during photoreaction. Roales et al. reported that it was possible to suppress the aggregation of porphyrin moiety by selecting an anchor group vertically fixed on TiO_2.[79] Thus, the pyridyl anchor groups of 2 are vertically fixed to the TiO_2 surface to produce small changes in the absorption spectrum during photoreaction.

Ooyama et al. reported that a cyclic porphyrin dimer with pyridyl anchors exhibited Brønsted acid-type interactions on TiO_2 in a dye-sensitized solar cell system.[76] Figures 6d−f present the FT-IR spectra of the dye/1 wt % Pt−TiO and $^{-2}$ bulk 1 3. All the bulk dyes exhibited pyridine C N stretching vibration peaks at 1592−1593 cm^{-1}. After loading the dyes onto 1 wt % Pt−TiO_2, the peaks were observed to shift by approximately 3−5 cm^{-1} to 1595−1597 cm^{-1}, indicating that the pyridyl groups established a hydrogen bond with the Brønsted acid sites on the TiO_2 surface; further, new peaks were observed at 1652−1653 cm^{-1}, which indicated the occurrence of this pyridinium behavior. After exposure to visible light, all these peaks remained unchanged in the FT-IR spectra, indicating that the pyridyl group−Brønsted acid-type interaction helped to stabilize the dye on TiO_2 during the photocatalytic reaction.

Photocurrent Spectra of Dyes on 1 wt % Pt−TiO_2 Films. In these porphyrin systems, the observed LUMO energy levels of dyes 1−3 were higher than those of the conduction band of TiO_2 (Figure 4). The dyes were selectively excited by visible light, and electrons were injected from the excited states of the dyes to the TiO_2 surface.[52] Hua et al. measured the photocurrent using a dye-loaded TiO_2 thin film applied to FTO and reported that the catalytic system displayed an efficient interfacial electron transfer from the dye to TiO_2, which provided the conditions for a high rate of hydrogen production.[80] To confirm the dye−sensitizer mechanism and differences in interfacial electron transfer for 1−3 during photocatalytic hydrogen production, the photo-currents of 1−3/1 wt % Pt−TiO_2 films on FTO were measured. Figure 7 depicts the photocurrent plots under irradiation by visible light (>420 nm) for 1−3/1 wt % Pt− TiO_2/ FTO films at 0 V (vs Ag/AgCl. 0.1 M Na_2SO_4 aq.). All the dye-containing films generated a higher current than that of

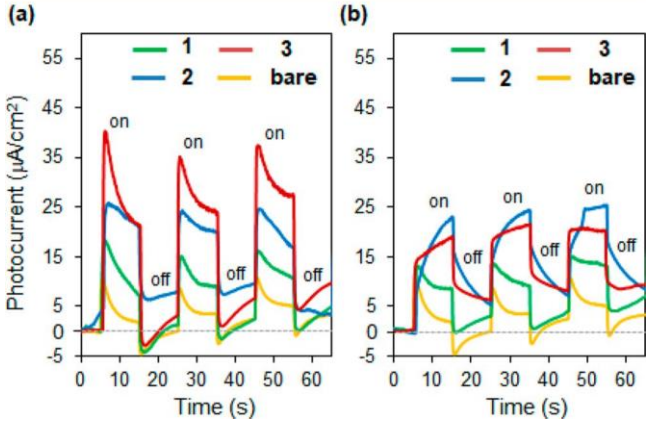

Figure 7. Photocurrent plots of dye/1 wt % Pt-loaded TiO_2/ FTO and bare (1 wt % Pt-loaded TiO_2/ FTO): (a) before and (b) after visible light-driven hydrogen production. Amperometric i−t curve at 0 V (vs Ag/AgCl. 0.1 M Na_2SO_4 aq. (pH 4), Pt counter electrode).

the bare Pt−TiO_2/ FTO film, confirming the occurrence of the visible light-driven dye-sensitized electron injection into 1 wt % Pt-loaded TiO_2/FTO. The absorption properties of those porphyrin dyes were in contrast to their photocatalytic activities. Before conducting the photocatalytic hydrogen production test, the order of photocurrent strength was 3 > 2 > 1; however, it was subsequently changed to 2 > 3 > 1 after the photocatalytic test. The photocurrent of the film containing 1 and 3 decreased, while a similar current was observed in the film containing 2. As depicted in Figures 6a−c, the spectral features of 1 and 3 also changed after the photocatalytic reaction, which was indicative of dye aggregation on the TiO_2 surface, resulting in a decrease in both the absorbance at the Soret band because of H-aggregation-type interaction and the photocurrent intensity. However, the absorption spectrum and photocurrent of 2 remained the same during photoreaction. Because of its high stability, dimer 2 demonstrated the highest hydrogen production performance. The rate of dye-sensitized hydrogen production was dependent on the amount of electrons that can be injected from the dye-sensitizer to the reaction site. These results indicated that the dye orientation strongly affected the electron injection efficiency from the organic dye to the TiO_2 surface.

On the basis of these photocatalytic tests and photocurrent results, the excited state of dyes 1−3 was observed to result in the injection of electrons from the dye to the TiO_2 surface. As depicted in Figure 8, under visible-light (>420 nm) irradiation,

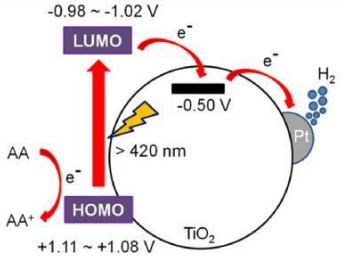

Figure 8. Proposed mechanism for photocatalytic H_2 generation in the dye 1−3/Pt/TiO_2 system under visible-light irradiation.

the electrons in the HOMOs of 1−3 (+1.08 to +1.11 V vs NHE) were excited to the LUMOs (−0.98 to −1.02 V vs NHE), creating excited-state dyes 1−3. The potentials of LUMOs were more negative than the CB of TiO_2 (−0.50 V vs NHE), thus providing a suitable thermodynamic driving force for electron injection from the excited state of 1−3 to TiO_2. The injected electrons migrate to the platinum (Pt) cocatalyst, which results in the effective production of hydrogen. The oxidized dye $(1-3)^+$ exhibits a higher oxidation potential than that exhibited by ascorbic acid (AA, +0.46 vs NHE)[81] and can be regenerated by reduction with AA. TiO_2 acts as the electron transfer bridge between the dye and the Pt cocatalyst on TiO_2, effectively causing the charge separation and photocatalytic hydrogen production that are observed in the dye/Pt−TiO_2−AA system.

CONCLUSIONS

The monomer, dimer, and trimer of 5,15-diphenyl-10,20-di(pyridin-4-yl)porphyrin were used to investigate the multi-anchoring effect on 1 wt % Pt−TiO_2 for visible light-driven photocatalytic hydrogen production in water. The dimer

system exhibited optimal hydrogen production characteristics, high stability over an 80-h period, and a superior production rate of 1023 μmol·g^{-1}·h^{-1}. The hydrogen production rates for the trimer and monomer were 723 and 123 μmol·g^{-1}·h^{-1}, respectively. These pyridyl groups were anchored on the TiO_2 surface through Brønsted acid-type hydrogen bonding in which the coordination prevented the dissociation of the dye from the TiO_2 surface. The dimer and trimer demonstrated a smaller amount of dye dissociation after the photoreaction as compared to that demonstrated by the monomer, indicating that the multiple pyridyl−TiO_2 interactions enhanced the stability of the dye-sensitized photocatalytic system. The absorption spectra and photocurrents of the monomer and trimer indicated that the dye arrangements and orientations were altered during photoreaction, while the dimer of the more rigid structure displayed virtually no change. Consequently, the high stability of the dimer on TiO_2 achieved the highest hydrogen production activity. The results of this study revealed the positive effects of employing the multianchoring of pyridyl−TiO_2 on effective hydrogen production by yielding a highly stable photocatalytic system for artificial photosynthesis. This approach can pave the way for further developing new and highly stable dye-sensitized photocatalysts.

EXPERIMENTAL SECTION

General Information. The ^{1}H spectrum was recorded on a Bruker AV600 (600 MHz) spectrometer. The ^{1}H NMR chemical shifts were reported to be δ values (ppm) relative to Me_4Si. The high-resolution FAB mass spectra were recorded on a JMS-700 MS station spectrometer. The FAB-MS spectra were measured using 3-nitro-benzyl alcohol (NBA) as the matrix. Analytical thin layer chromatography (TLC) was performed on Merck silica gel 60 F254, while flash column chromatography was performed using Kanto Si60N (neutral) silica gel. The absorption and diffuse reflectance spectra were recorded on a Shimadzu UV-3600. The diffuse reflectance spectra of the catalyst were measured with 1 wt % catalyst-loaded $BaSO_4$ pellets. The BET surface area was measured on a BELSORP-max-32-N-VP-CM (MicrotracBEL Corp.). The IR spectra were recorded on a Shimadzu IR Prestige-21 spectrophotometer. All the solvents and reagents were of reagent quality, purchased commercially, and used as received without further purification. The FTO overlayer conducting glass (transmission >90% in the visible, sheet resistance 7 Ω square^{-1} was purchased from Sigma-Aldrich. Titanium-oxide paste of Ti-Nanoxide T/SP was purchased from Solaronix.

Dye-Loading Process into 1 wt % Pt-Loaded TiO_2 Anatase. The preparation method for 1.0 wt % Pt-loaded TiO_2 was observed to be as follows in accordance with the literature.[36,38] The commercially available TiO_2 (<25 nm, anatase, Aldrich) was used. 1.0 wt % Pt-loaded TiO_2 (50 mg) was immersed in a 1,1,2,2-tetrachloroethane solution containing dye sensitizers (3×10^{-4} M, 10 mL) at room temperature for 24 h in the dark. The amount of dye-loading was estimated by obtaining the difference of absorption intensity at the Soret band before and after the absorption spectra.[82] On the basis of the calibration curve, the dye-loading amount on 1 wt % Pt/TiO_2 was estimated for 1 (8.2 μmol/g), 2 (28.3 μmol/g), and 3 (30.1 μmol/g). After the 1 wt % Pt/TiO_2 was dye-loaded, the solvent was eliminated by centrifugation (3600 rpm, 20 min). The catalyst was recovered by filtration and rinsed using 1,1,2,2-tetrachloroethane. The dye-loaded 1.0 wt % Pt-loaded TiO_2 catalyst powder was dried under vacuum at room temperature and was further used to perform the water splitting reactions without conducting any further treatment.

Photocatalytic Hydrogen Production Reaction. The photocatalytic hydrogen production experiment was performed using a conventional closed-circulation system with a dead volume of approximately 500 mL. The Pt/dye/TiO_2 catalyst (10 mg) was suspended in 10 mL of ascorbic acid water (pH 4.0, adjusted using NaOH aq.). A quartz reaction cell was irradiated using a 300 W Xe lamp (Asahi Inc., Japan) equipped with a cutoff filter that was less than 420 nm (Edmund optics, >420 nm cutoff). During the H_2O photochemical reaction, the mixture was magnetically stirred. The amount of obtained H_2 gas was measured using a thermal conductivity detector gas chromatograph (GC-8A, Shimadzu Corp., Japan) that was connected to a conventional volumetric circulation line with a vacuum pump. The photoreaction film (dye-loaded 1 wt % Pt−TiO_2 film/FTO substrate) experiments were performed using the same reaction cell and conditions, except for the fact that 30 mL of ascorbic acid water (pH 4.0, adjusted using NaOH aq.) was used.

Fabrication of the 1 wt %-Co-loaded TiO_2/FTO Substrate and Photocurrent Spectra. The Pt source was used as chloroplatinic acid solution of 8 wt % in water (Sigma-Aldrich). The preparation of the anatase phase thin-film has been described elsewhere.[83] A thin film of 1 wt % Pt-co-loaded−TiO_2 was prepared to coat an FTO glass substrate, with the dimensions of the active area being controlled at 1.5 cm^2. The photocurrent was measured using a BAS ALS1200B instrument. All the measurements were performed in DI water solutions containing 0.1 M Na_2SO_4 as a supporting electrolyte, where pH = 4. A conventional three electrode configuration (dye-loaded 1 wt % Pt−TiO_2 film/FTO substrate working electrode, platinum mesh counter electrode, and Ag/AgCl reference electrode) was employed. The photocurrent properties were obtained under irradiation by a 300 W Xe lamp (Asahi Spectra, MAX-303) using a long-pass filter (Edmund optics, > 420 nm cutoff).

Synthesis of Cyclic Trimer 3. A mixture of zinc(II) 5,15-bis(3-ethynylphenyl)-10,20-di(pyridin-4-yl)porphyrin (292 mg, 0.4 mmol), CuCl (4.0 g, 40 mmol), and pyridine (300 mL) was heated at 85 °C for 12 h. The mixture was further cooled to 0 °C, and 7 M NH_3 aq. (150 mL) was added. Oxygen was bubbled through the reaction mixture for 30 min at 0 °C. The mixture was further extracted with $CHCl_3$, washed with 7 M NH_3 aq. three times, and concentrated to dryness. The residual solid was dissolved in $CHCl_3$ (200 mL), and a minimum amount of pyridine (~1 mL) and 6 M HCl (40 mL) was added. The solution was allowed to react for 30 min. The solution was further neutralized with sat. $NaHCO_3$ aq. and dried over anhydrous Na_2SO_4. Purification with flash chromatography (gradient elution $CHCl_3$:EtOH = 100:1 to 10:1) yielded 2 (21.6 mg, 8%) and the target compound 3 (52.4 mg, 20%) as a purple-red solid. Physical data of 3: mp > 300 °C; ^{1}H NMR (CCl_3, 600 MHz) −3.05 (bs, 6H), 7.71−8.00 (m, 6H), 8.03−8.23 (m, 30H), 8.73−8.98 (m, 36H); a clear ^{13}C NMR spectrum of 3 could not be obtained due to the low solubility; ν(ATR) 1592 (C = N) cm^{-1}; HRMS (FAB) m/z $[M + H]^+$ calculated for $C_{138}H_{79}N_{18}$ 1987.6735; found 1987.6728.

ASSOCIATED CONTENT

Absorption spectra of dyes on TiO_2 film, difference pulse voltammetry of 1−3, 0.1 M nBu_4NPF_6 in 1,1,2,2-tetrachloroethane solution, absorption spectra of soluble species in 1,1,2,2-tetrachloroethane solvent from an aqueous solution after the photocatalytic hydrogen production reaction, the time-course of the turnover numbers per porphyrin unit for hydrogen production, and visible light-driven photocatalytic hydrogen produc-tion under dye/Pt−TiO_2 film in FTO substrate conditions (PDF)

AUTHOR INFORMATION

Corresponding Authors
*E-mail: mwata@i2cner.kyushu-u.ac.jp.
*E-mail: tanif@ms.ifoc.kyushu-u.ac.jp.

ORCID

Motonori Watanabe: 0000-0003-3621-4361
Songmei Sun: 0000-0001-9545-9073
Fumito Tani: 0000-0002-9166-2127

Notes

The authors declare no competing financial interest.

ACKNOWLEDGMENTS

This study were supported by Grant-in-Aids for Science Research (17H04888 and 15K05432) from the Ministry of Education, Culture, Sports, Science and Technology (MEXT), Japan and the Strategic International Collaborative Research Program (SICORP) in "Research on Hydrogen as a renewable energy carrier" from Japan Science and Technology Agency (JST), Japan, and was performed under the Cooperative Research Program of "Network Joint Research Centre for Materials and Devices" (IMCE, Kyushu University). M.W. and S.M.S. acknowledge the support from I2CNER, funded by the World Premier International Research Centre Initiative (WPI), MEXT, Japan.

REFERENCES

(1) Hirano, K.; Suzuki, E.; Ishikawa, A.; Moroi, T.; Shiroishi, H.; Kaneko, M. Sensitization of TiO_2 Particles by Dyes to Achieve H_2 Evolution by Visible Light. J. Photochem. Photobiol., A 2000, 136, 157−161.

(2) Zhang, X.; Veikko, U.; Mao, J.; Cai, P.; Peng, T. Visible-Light-Induced Photocatalytic Hydrogen Production Over Binuclear Ru^{II}− bipyridyl Dye-Sensitized TiO_2 Without Noble Metal Loading. Chem. - Eur. J. 2012, 18, 12103−12111.

(3) Kim, W.; Tachikawa, T.; Majima, T.; Li, C.; Kim, H.-J.; Choi, W. Tin-Porphyrin Sensitized TiO_2 for the Production of H_2 Under Visible Light. Energy Environ. Sci. 2010, 3, 1789−1795.

(4) Hasobe, T.; Sakai, H.; Mase, K.; Ohkubo, K.; Fukuzumi, S. Remarkable Enhancement of Photocatalytic Hydrogen Evolution Efficiency Utilizing an Internal Cavity of Supramolecular Porphyrin Hexagonal Nanocylinders Under Visible-Light Irradiation. J. Phys. Chem. C 2013, 117, 4441−4449.

(5) Gurunathan, K.; Maruthamuthu, P.; Sastri, M. Photocatalytic Hydrogen Production by Dye-Sensitized Pt/SnO_2 and Pt/SnO_2/RuO_2 in Aqueous Methyl Viologen Solution. Int. J. Hydrogen Energy 1997, 22, 57−62.

(6) Shimidzu, T.; Iyoda, T.; Koide, Y. An Advanced Visible-Light-Induced Water Reduction with Dye-Sensitized Semiconductor Powder Catalyst. J. Am. Chem. Soc. 1985, 107, 35−41.

(7) Jin, Z. L.; Zhang, X. J.; Li, Y. X.; Li, S. B.; Lu, G. X. 5.1% Apparent Quantum Efficiency for Stable Hydrogen Generation Over Eosin-Sensitized CuO/TiO_2 Photocatalyst Under Visible Light Irradiation. Catal. Commun. 2007, 8, 1267−1273.

(8) Hagiwara, H.; Ono, N.; Inoue, T.; Matsumoto, H.; Ishihara, T. Dye- Sensitizer Effects on a Pt/KTa(Zr)O_3 Catalyst for the Photocatalytic Splitting of Water. Angew. Chem., Int. Ed. 2006, 45, 1420−1422.

(9) Hagiwara, H.; Inoue, T.; Kaneko, K.; Ishihara, T. Charge-Transfer Mechanism in Pt/KTa(Zr)O_3 Photocatalysts Modified with Porphyrinoids for Water Splitting. Chem. - Eur. J. 2009, 15, 12862− 12870.

(10) Hagiwara, H.; Higashi, K.; Watanabe, M.; Kakigi, R.; Ida, S.; Ishihara, T. Effect of Porphyrin Molecular Structure on Water Splitting Activity of a $KTaO_3$ Photocatalyst. Catalysts 2016, 6, 42.

(11) Hagiwara, H.; Nagatomo, M.; Seto, C.; Ida, S.; Ishiahara, T. Dye Modification Effects on TaON for Photocatalytic Hydrogen Production from Water. Catalysts 2013, 3, 614−624.

(12) Hagiwara, H.; Watanabe, M.; Daio, T.; Ida, S.; Ishihara, T. Modification Effects of Meso-Hexakis(pentafluorophenyl) [26]-Hexaphyrin Aggregates on the Photocatalytic Water Splitting. Chem. Commun. 2014, 50, 12515−12518.

(13) Zhang, L.; Wang, W. Z.; Sun, S. M.; Sun, Y. Y.; Gao, E.; Xu, J. Water Splitting from Dye Wastewater: A Case Study of BiOCl/ Copper(II) Phthalocyanine Composite Photocatalyst. Appl. Catal., B 2013, 132-133, 315−320.

(14) Maeda, K.; Eguchi, M.; Youngblood, W. J.; Mallouk, T. E. Niobium Oxide Nanoscrolls as Building Blocks for Dye-Sensitized Hydrogen Production from Water Under Visible Light Irradiation. Chem. Mater. 2008, 20, 6770−6778.

(15) Maeda, K.; Eguchi, M.; Lee, S. H. A.; Youngblood, W. J.; Hata, H.; Mallouk, T. E. Photocatalytic Hydrogen Evolution from Hexaniobate Nanoscrolls and Calcium Niobate Nanosheets Sensitized by Ruthenium (II) Bipyridyl Complexes. J. Phys. Chem. C 2009, 113, 7962−7969.

(16) Abe, R.; Sayama, K.; Arakawa, H. Dye-Sensitized Photocatalysts for Efficient Hydrogen Production from Aqueous I^- Solution Under Visible Light Irradiation. J. Photochem. Photobiol., A 2004, 166, 115− 122.

(17) Abe, R.; Shinmei, K.; Koumura, N.; Hara, K.; Ohtani, B. Visible-Light-Induced Water Splitting Based on Two-Step Photo-excitation Between Dye-Sensitized Layered Niobate and Tungsten Oxide Photocatalysts in the Presence of a Triiodide/Iodide Shuttle Redox Mediator. J. Am. Chem. Soc. 2013, 135, 16872−16884.

(18) Zhu, M. S.; Dong, Y. P.; Xiao, B.; Du, Y. K.; Yang, P.; Wang, X. M. Enhanced Photocatalytic Hydrogen Evolution Performance Based on Ru-Trisdicarboxybipyridine-Reduced Graphene Oxide Hybrid. J. Mater. Chem. 2012, 22, 23773−23779.

(19) Gong, X.; Liu, G.; Li, Y.; Yu, D. Y. W.; Teoh, W. Y. Functionalized-Graphene Composites: Fabrication and Applications in Sustainable Energy and Environment. Chem. Mater. 2016, 28, 8082−8118.

(20) Min, S. X.; Lu, G. X. Dye-Sensitized Reduced Graphene Oxide Photocatalysts for Highly Efficient Visible-Light-Driven Water Reduction. J. Phys. Chem. C 2011, 115, 13938−13945.

(21) Mou, Z. G.; Dong, Y. P.; Li, S. J.; Du, Y. K.; Wang, X. M.; Yang, P.; Wang, S. D. Eosin Y Functionalized Graphene for Photocatalytic Hydrogen Production from Water. Int. J. Hydrogen Energy 2011, 36, 8885−8893.

(22) Ge, Li.; Li, X.; Kang, S.-Z.; Qin, L.; Li, G. Highly Efficient Graphene Oxide/Porphyrin Photocatalysts for Hydrogen Evolution and the Interfacial Electron Transfer. Appl. Catal., B 2016, 187, 67− 74.

(23) Wang, Y. B.; Hong, J. D.; Zhang, W.; Xu, R. Carbon Nitride Nanosheets for Photocatalytic Hydrogen Evolution: Remarkably Enhanced Activity by Dye Sensitization. Catal. Sci. Technol. 2013, 3, 1703−1711.

(24) Xu, J. Y.; Li, Y. X.; Peng, S. Q. Photocatalytic Hydrogen Evolution Over Erythrosin B-Sensitized Graphitic Carbon Nitride with in Situ Grown Molybdenum Sulfide Cocatalyst. Int. J. Hydrogen Energy 2015, 40, 353−362.

(25) Zhang, X. H.; Peng, B.; Zhang, S.; Peng, T. Y. Robust Wide Visible-Light-Responsive Photoactivity for H_2 Production Over a Polymer/Polymer Heterojunction Photocatalyst: The Significance of Sacrificial Reagent. ACS Sustainable Chem. Eng. 2015, 3, 1501−1509.

(26) Zhang, X.; Peng, T.; Song, S. Recent Advances in Dye-Sensitized Semiconductor Systems for Photocatalytic Hydrogen Production. J. Mater. Chem. A 2016, 4, 2365−2402.

(27) Takanabe, K.; Kamata, K.; Wang, X. C.; Antonietti, M.; Kubota, J.; Domen, K. Photocatalytic Hydrogen Evolution on Dye-Sensitized Mesoporous Carbon Nitride Photocatalyst with Magnesium Phtha-locyanine. Phys. Chem. Chem. Phys. 2010, 12, 13020−13025.

(28) Huang, J.; Wu, Y. J.; Wang, D. D.; Ma, Y. F.; Yue, Z. K.; Lu, Y. T.; Zhang, M. X.; Zhang, Z. J.; Yang, P. Silicon Phthalocyanine Covalently Functionalized N-Doped Ultrasmall Reduced Graphene Oxide Decorated with Pt Nanoparticles for Hydrogen Evolution from Water. ACS Appl. Mater. Interfaces 2015, 7, 3732−3741.

(29) Wang, D. D.; Huang, J.; Li, X.; Yang, P.; Du, Y. K.; Goh, C. M.; Lu, C. Photocatalytic H_2 Production Under Visible-Light Irradiation

Based on Covalent Attachment of Manganese Phthalocyanine to Graphene. J. Mater. Chem. A 2015, 3, 4195−4202.
(30) Li, Y. X.; Guo, M. M.; Peng, S. Q.; Lu, G. X.; Li, S. B. Formation of Multilayer-Eosin Y-Sensitized TiO_2 via Fe^{3+} Coupling for Efficient Visible-Light Photocatalytic Hydrogen Evolution. Int. J. Hydrogen Energy 2009, 34, 5629−5636.
(31) Min, S. X.; Lu, G. X. Dye-Cosensitized Graphene/Pt Photocatalyst for High Efficient Visible Light Hydrogen Evolution. Int. J. Hydrogen Energy 2012, 37, 10564−10574.
(32) Le, T. T.; Akhtar, M. S.; Park, D. M.; Lee, J. C.; Yang, O. B. Water Splitting on Rhodamine-B Dye Sensitized Co-Doped TiO_2 Catalyst Under Visible Light. Appl. Catal., B 2012, 111-112, 397−401.
(33) Zhang, W. Y.; Li, Y. X.; Zeng, X. P.; Peng, S. Q. Synergetic Effect of Metal Nickel and Graphene as a Cocatalyst for Enhanced Photocatalytic Hydrogen Evolution via Dye Sensitization. Sci. Rep. 2015, 5, 10589.
(34) Cecconi, B.; Manfredi, N.; Montini, T.; Fornasiero, P.; Abbotto, A. Dye-Sensitized Solar Hydrogen Production: The Emerging Role of Metal- Free Organic Sensitizers. Eur. J. Org. Chem. 2016, 2016, 5194−5215.
(35) Swetha, T.; Mondal, I.; Bhanuprakash, K.; Pal, U.; Singh, S. P. First Study on Phosphonite-Coordinated Ruthenium Sensitizers for Efficient Photocatalytic Hydrogen Evolution. ACS Appl. Mater. Interfaces 2015, 7, 19635−19642.
(36) Watanabe, M.; Hagiwara, H.; Iribe, A.; Ogata, Y.; Shiomi, K.; Staykov, A.; Ida, S.; Tanaka, K.; Ishihara, T. Spacer Effects in Metal-Free Organic Dyes for Visible-Light-Driven Dye-Sensitized Photo-catalytic Hydrogen Production. J. Mater. Chem. A 2014, 2, 12952− 12961.
(37) Lee, J.; Kwak, J.; Ko, K. C.; Park, J. H.; Ko, J. H.; Park, N.; Kim, E.; Ryu, D. H.; Ahn, T. K.; Lee, J. Y.; Son, S. U. Phenothiazine-Based Organic Dyes with Two Anchoring Groups on TiO_2 for Highly Efficient Visible Light-Induced Water Splitting. Chem. Commun. 2012, 48, 11431−11433.
(38) Watanabe, M.; Hagiwara, H.; Ogata, Y.; Staykov, A.; Bishop, S. R.; Perry, N. H.; Chang, Y. J.; Ida, S.; Tanaka, K.; Ishihara, T. Impact of Alkoxy Chain Length on Carbazole-Based, Visible Light-Driven, Dye Sensitized Photocatalytic Hydrogen Production. J. Mater. Chem. A 2015, 3, 21713−21721.
(39) Han, W.-S.; Wee, K.-R.; Kim, H.-Y.; Pac, C.; Nabetani, Y.; Yamamoto, D.; Shimada, T.; Inoue, H.; Choi, H.; Cho, K.; Kang, S. O. Hydrophilicity Control of Visible- Light Hydrogen Evolution and Dynamics of the Charge- Separated State in Dye/TiO_2/Pt Hybrid Systems. Chem. - Eur. J. 2012, 18, 15368−15381.
(40) Li, Q.; Che, Y.; Ji, H.; Chen, C.; Zhu, H.; Ma, W.; Zhao, J. Ortho-Dihydroxyl-9,10-Anthraquinone Dyes as Visible-Light Sensi-tizers that Exhibit a High Turnover Number for Hydrogen Evolution. Phys. Chem. Chem. Phys. 2014, 16, 6550−6554.
(41) Tiwari, A.; Pal, U. Effect of Donor-Donor-π-Acceptor Architecture of Triphenylamine-Based Organic Sensitizers Over TiO_2 Photocatalysts for Visible-Light-Driven Hydrogen Production. Int. J. Hydrogen Energy 2015, 40, 9069−9079.
(42) Choi, S. K.; Yang, H. S.; Kim, J. H.; Park, H. Organic Dye-Sensitized TiO_2 as a Versatile Photocatalyst for Solar Hydrogen and Environmental Remediation. Appl. Catal., B 2012, 121-122, 206−213.
(43) Tiwari, A.; Mondal, I.; Pal, U. Visible Light Induced Hydrogen Production Over Thiophenothiazine-Based Dye Sensitized TiO_2 Photocatalyst in Neutral Water. RSC Adv. 2015, 5, 31415−31421.
(44) Manfredi, N.; Cecconi, B.; Calabrese, V.; Minotti, A.; Peri, F.; Ruffo, R.; Monai, M.; Romero-Ocana, I.; Montini, T.; Fornasiero, P.; Abbotto, A. Dye-Sensitized Photocatalytic Hydrogen Production: Distinct Activity in a Glucose Derivative of a Phenothiazine Dye. Chem. Commun. 2016, 52, 6977−6980.
(45) Youngblood, W. J.; Lee, S.-H. A.; Kobayashi, Y.; Hernandez-Pagan, E. A.; Hoertz, P. G.; Moore, T. A.; Moore, A. L.; Gust, D.; Mallouk, T. E. Photoassisted Overall Water Splitting in a Visible Light-Absorbing Dye-Sensitized Photoelectrochemical Cell. J. Am. Chem. Soc. 2009, 131, 926−927.
(46) Kuriki, R.; Maeda, K. Development of Hybrid Photocatalysts Constructed with a Metal Complex and Graphitic Carbon Nitride for Visible-Light-Driven CO_2 Reduction. Phys. Chem. Chem. Phys. 2017, 19, 4938−4950.
(47) Maeda, K.; Sahara, G.; Eguchi, M.; Ishitani, O. Hybrids of a Ruthenium(II) Polypyridyl Complex and a Metal Oxide Nanosheet for Dye-Sensitized Hydrogen Evolution with Visible Light: Effects of the Energy Structure on Photocatalytic Activity. ACS Catal. 2015, 5, 1700−1707.
(48) Ikeda, S.; Abe, C.; Torimoto, T.; Ohtani, B. Photochemical Hydrogen Evolution from Aqueous Triethanolamine Solutions Sensitized by Binaphthol-Modified Titanium(IV) Oxide Under Visible-Light Irradiation. J. Photochem. Photobiol., A 2003, 160, 61− 67.
(49) Kamegawa, T.; Matsuura, S.; Seto, H.; Yamashita, H. A Visible-Light-Harvesting Assembly with a Sulfocalixarene Linker Between Dyes and a Pt-TiO_2 Photocatalyst. Angew. Chem., Int. Ed. 2013, 52, 916−919.
(50) Zhang, G.; Choi, W. A Low-Cost Sensitizer Based on a Phenolic Resin for Charge-Transfer Type Photocatalysts Working Under Visible Light. Chem. Commun. 2012, 48, 10621−10623.
(51) Bae, R.; Choi, W. Effect of the Anchoring Group (Carboxylate vs Phosphonate) in Ru-Complex Sensitized TiO_2 on Hydrogen Production Under Visible Light. J. Phys. Chem. B 2006, 110, 14792− 14799.
(52) Watanabe, M. Dye-Sensitized Photocatalyst for Effective Water Splitting Catalyst. Sci. Technol. Adv. Mater. 2017, 18, 705−723.
(53) Cecconi, B.; Manfredi, N.; Ruffo, R.; Montini, T.; Romero-Ocaña, I.; Fornasiero, P.; Abbotto, A. Tuning Thiophene-Based Phenothiazines for Stable Photocatalytic Hydrogen Production. ChemSusChem 2015, 8, 4216−4228.
(54) Zhang, L.; Cole, J. M. Anchoring Groups for Dye-Sensitized Solar Cells. ACS Appl. Mater. Interfaces 2015, 7, 3427−3455.
(55) Liu, F.-S.; Ji, R.; Wu, M.; Sun, Y.-M. Hydrogen Production from Water Splitting Using Perylene Dye-Sensitized Pt/TiO_2 Photocatalyst. Acta Phys. Chim. Sin. 2007, 23, 1899.
(56) Takijiri, K.; Morita, K.; Nakazono, T.; Sakai, K.; Ozawa, H. Highly Stable Chemisorption of Dyes with Pyridyl Anchors over TiO_2: Application in Dye-Sensitized Photoelectrochemical Water Reduction in Aqueous Media. Chem. Commun. 2017, 53, 3042−3045.
(57) Maitani, M. M.; Zhan, C. H.; Mochizuki, D.; Suzuki, E.; Wada, Y. Influence of Co-Existing Species on Charge Transfer in Dye-Sensitized Nanocrystalline Oxide Semiconductors in Aqueous Suspension for H_2 Evolution Under Visible Light. Appl. Catal., B 2014, 147, 770−778.
(58) Maitani, M. M.; Zhan, C. H.; Mochizuki, D.; Suzuki, E.; Wada, Y. Influence of Co-Existing Alcohol on Charge Transfer of H_2 Evolution Under Visible Light with Dye-Sensitized Nanocrystalline TiO_2. Appl. Catal., B 2013, 140−141, 406−411.
(59) Zhang, N.; Wang, L.; Wang, H.; Cao, R.; Wang, J.; Bai, F.; Fan, H. Self-Assembled One-Dimensional Porphyrin Nanostructures with Enhanced Photocatalytic Hydrogen Generation. Nano Lett. 2018, 18, 560−566.
(60) Zhu, M.; Li, Z.; Xiao, B.; Lu, Y.; Du, Y.; Yan, P.; et al. Surfactant Assistance in Improvement of Photocatalytic Hydrogen Production with the Porphyrin Noncovalently Functionalized Graphene Nanocomposite. ACS Appl. Mater. Interfaces 2013, 5, 1732−1740.
(61) Yuan, Y.-J.; Chen, D.; Zhong, J.; Yang, L.-X.; Wang, J.-J.; Yu, Z.-T.; Zou, Z.-G. Construction of a Noble-Metal-Free Photocatalytic H_2 Evolution System Using MoS_2/Reduced Graphene Oxide Catalyst and Zinc Porphyrin Photosensitizer. J. Phys. Chem. C 2017, 121, 24452−24462.
(62) Wang, D. H.; Pan, J. N.; Li, H. H.; Liu, J. J.; Wang, Y. B.; Kang, L. T.; Yao, J. N. A Pure Organic Heterostructure of μ-Oxo Dimericiron (III) Porphyrin and Graphitic-C_3N_4 for Solar H_2 Production from Water. J. Mater. Chem. A 2016, 4, 290−296.
(63) Mei, S.; Gao, J.; Zhang, Y.; Yang, J.; Wu, Y.; Wang, X.; Zhao, R.; Zhai, X.; Hao, C.; Li, R.; Yan, J. Enhanced Visible Light

Photocatalytic Hydrogen Evolution Over Porphyrin Hybridized Graphitic Carbon Nitride. J. Colloid Interface Sci. 2017, 506, 58−65.

(64) Wang, J.; Zheng, Y.; Peng, T.; Zhang, J.; Li, R. Asymmetric Zinc Porphyrin Derivative-Sensitized Graphitic Carbon Nitride for Efficient Visible-Light-Driven H_2 Production. ACS Sustainable Chem. Eng. 2017, 5, 7549−7556.

(65) Yuan, Y.; Lu, H.; Ji, Z.; Zhong, J.; Ding, M.; Chen, D.; Li, Y.; Tu, W.; Cao, D.; Yu, Z.; Zou, Z. Enhanced Visible-Light-Induced Hydrogen Evolution from Water in a Noble-Metal-Free System Catalyzed by ZnTCPP-MoS_2/TiO_2 Assembly. Chem. Eng. J. 2015, 275, 8−16.

(66) Yuan, Y.-J.; Tu, J.-R.; Ye, Z.-J.; Lu, H.-W.; Ji, Z.-G.; Hu, B.; Li, Y.-H.; Cao, D.-P.; Yu, Z.-T.; Zou, Z.-G. Visible-Light-Driven Hydrogen Production from Water in a Noble-Metal-Free System Catalyzed by Zinc Porphyrin Sensitized MoS_2/ZnO. Dyes Pigm. 2015, 123, 285−292.

(67) Nobukuni, H.; Shimazaki, Y.; Tani, F.; Naruta, Y. A Nanotube of Cyclic Porphyrin Dimers Connected by Nonclassical Hydrogen Bonds and Its Inclusion of C_{60} in a Linear Arrangement. Angew. Chem., Int. Ed. 2007, 46, 8975−8978.

(68) Nobukuni, H.; Tani, F.; Shimazaki, Y.; Naruta, Y.; Ohkubo, K.; Nakanishi, T.; Kojima, T.; Fukuzumi, S.; Seki, S. Anisotropic High Electron Mobility and Photodynamics of a Self-Assembled Porphyrin Nanotube Including C_{60} Molecules. J. Phys. Chem. C 2009, 113, 19694−19699.

(69) Kamimura, T.; Ohkubo, K.; Kawashima, Y.; Nobukuni, H.; Naruta, Y.; Tani, F.; Fukuzumi, S. Submillisecond-Lived Photo-induced Charge Separation in Inclusion Complexes Composed of Li^+@C_{60} and Cyclic Porphyrin Dimers. Chem. Sci. 2013, 4, 1451− 1461.

(70) Sakaguchi, K.; Kamimura, T.; Uno, H.; Mori, S.; Ozako, S.; Nobukuni, H.; Ishida, M.; Tani, F. Phenothiazine-Bridged Cyclic Porphyrin Dimers as High-Affinity Hosts for Fullerenes and Linear Array of C_{60} in Self-Assembled Porphyrin Nanotube. J. Org. Chem. 2014, 79, 2980−2992.

(71) Kamimura, T.; Ohkubo, K.; Kawashima, Y.; Ozako, S.; Sakaguchi, K.; Fukuzumi, S.; Tani, F. Long-Lived Photoinduced Charge Separation in Inclusion Complexes Composed of a Phenothiazine-Bridged Cyclic Porphyrin Dimer and Fullerenes. J. Phys. Chem. C 2015, 119, 25634−25650.

(72) Nishihara, H.; Hirota, T.; Matsuura, K.; Ohwada, M.; Hoshino, N.; Akutagawa, T.; Higuchi, T.; Jinnai, H.; Koseki, Y.; Kasai, H.; Matsuo, Y.; Maruyama, J.; Hayasaka, Y.; Konaka, H.; Yamada, Y.; Yamaguchi, S.; Kamiya, K.; Kamimura, T.; Nobukuni, H.; Tani, F. Synthesis of Ordered Carbonaceous Frameworks from Organic Crystals. Nat. Commun. 2017, 8, 109.

(73) Nobukuni, H.; Shimazaki, Y.; Uno, H.; Naruta, Y.; Ohkubo, K.; Kojima, T.; Fukuzumi, S.; Seki, S.; Sakai, H.; Hasobe, T.; Tani, F. Supramolecular Structures and Photoelectronic Properties of the Inclusion Complex of a Cyclic Free-Base Porphyrin Dimer and C_{60}. Chem. - Eur. J. 2010, 16, 11611−11623.

(74) Sakai, H.; Kamimura, T.; Tani, F.; Hasobe, T. Supramolecular Photovoltaic Cells Utilizing Inclusion Complexes Composed of Li^+@ C_{60} and Cyclic Porphyrin Dimer. J. Porphyrins Phthalocyanines 2015, 19, 242−250.

(75) Ooyama, Y.; Enoki, T.; Ohshita, J.; Kamimura, T.; Ozako, S.; Koide, T.; Tani, F. Singlet Oxygen Generation Properties of an Inclusion Complex of Cyclic Free-Base Porphyrin Dimer and Fullerene C_{60}. RSC Adv. 2017, 7, 18690−18695.

(76) Ooyama, Y.; Uenaka, K.; Kamimura, T.; Ozako, S.; Kanda, M.; Koide, T.; Tani, F. Dye-Sensitized Solar Cell Based on an Inclusion Complex of a Cyclic Porphyrin Dimer Bearing Four 4-Pyridyl Groups and Fullerene C_{60}. RSC Adv. 2016, 6, 16150−16158.

(77) Fleischer, E. B.; Shachter, A. M. Coordination Oligomers and a Coordination Polymer of Zinc Tetraarylporphyrins. Inorg. Chem. 1991, 30, 3763−3769.

(78) Pavlishchuk, V. V.; Addison, A. W. Conversion Constants for Redox Potentials Measured Versus Different Reference Electrodes in Acetonitrile Solutions at 25°C. Inorg. Chim. Acta 2000, 298, 97−102.

(79) Roales, J.; Pedrosa, J. M.; Guillen, M. G.; Lopes-Costa, T.; Castillero, P.; Barranco, A.; Gonzalez-Elipe, A. R. Free-Base Carboxyphenyl Porphyrin Films Using a TiO_2 Columnar Matrix: Characterization and Application as NO_2 Sensors. Sensors 2015, 15, 11118−11132.

(80) Yu, F.; Cui, S.-C.; Li, X.; Peng, Y.; Yu, Y.; Yun, K.; Zhang, S.-C.; Li, J.; Liu, J.-G.; Hua, J. Effect of Anchoring Groups on N-Annulated Perylene-Based Sensitizers for Dye-Sensitized Solar Cells and Photocatalytic H_2 Evolution. Dyes Pigm. 2017, 139, 7−18.

(81) Pati, P. B.; Damas, G.; Tian, L.; Fernandes, D. L. A.; Zhang, L.; Pehlivan, I. B.; Edvinsson, T.; Araujo, C. M.; Tian, H. An Experimental and Theoretical Study of an Efficient Polymer Nano-Photocatalyst for Hydrogen Evolution. Energy Environ. Sci. 2017, 10, 1372−1376.

(82) Chang, S.; Wang, H.; Hua, Y.; Li, Q.; Xiao, X.; Wong, W.-K.; Wong, W. Y.; Zhu, X.; Chen, T. Conformational Engineering of Co-Sensitizers to Retard Back Charge Transfer for High-Efficiency Dye-Sensitized Solar Cells. J. Mater. Chem. A 2013, 1, 11553−11558.

(83) Watanabe, M.; Uemura, N.; Ida, S.; Hagiwara, H.; Goto, K.; Ishihara, T. 5,5′-Alkylsubsituted Indigo for Solution-Processed Optoelectronic Devices. Tetrahedron 2016, 72, 4280−4287.